Electronic Supplementary Material (ESI) for RSC Advances.

Controllably fabricated polypyrrole nanorods network by doping tetra-β-carboxylate cobalt phthalocyanine tetrasodium salt for enhanced ammonia sensing at room temperature †

Shijie Gai[a], Xiaolin Wang[b], Runze Zhang[a], Kun Zeng[a], Shoulei Miao[a], Yiqun Wu[a,c], Bin Wang[*a]

[a] *Key Laboratory of Functional Inorganic Material Chemistry, Ministry of Education, School of Chemistry and Materials Science, Heilongjiang University, Harbin 150080, China*

[b] *School of Material and Chemical Engineering, Heilongjiang Institute of Technology, Harbin 150050, P. R. China*

[c] *Shanghai Institute of Optics and Fine Mechanics, Chinese Academy of Sciences, P.O. Box 800216, Shanghai 201800, China*

Experiment details

Materials:

1, 2, 4-Benzenetricarboxylic anhydride (97% purity) were purchased from Saan Chemical Technology (Shanghai) Co., Ltd. Ammonium molybdate tetrahydrate (purity ≥ 99%), urea (purity ≥ 99%) and Cobaltous (II) chloride hexahydrate (purity ≥ 99%) were purchased from Tianjin Kemiou Chemical Reagent Co., Ltd. All chemical reagents were of analytical grade and were no subsequent processing.

Synthesis of tetra-β-carboxylate cobalt phthalocyanine tetrasodium salt (TcCoPcTs).

Firstly, the tetra-β-amide cobalt phthalocyanine (TaCoPc) was synthesized by the traditional solid synthesis method. Subsequent substituent adjustments were made under alkaline and acidic conditions respectively [1]. The synthesis scheme is shown in **Scheme S1**.

12.90 g (0.067 mol) of 1,2,4-benzeneticarboxylicanhydride crushed into powder, 20.16 g (0.336 mol) of urea, 3.99 g (0.017 mol) of cobalt (II) chloride hexahydrate and 0.32 g (0.259 mmol) hexaammonium heptamolybdate tetrahydrate were evenly stirred mixed in three-necked bottle, the mixture powder gradually turned purple and slightly sticky. Then, the reaction system was kept at 160 °C in an oil bath, and the color of the system gradually changed from purple to blue. After the color no longer changed, the temperature was continued to rise to 230 °C for 7 h. After the reaction was completed and cooled to room temperature naturally, the product was washed with boiling water until the filtrate was colorless, then rinsed with methanol and acetone for several times, and finally dried in a vacuum oven at 60 °C for 6 h, blue-purple powder TaCoPc was obtained.

Secondly, 1.50 g of TaCoPc obtained from the above reaction was transferred to a three-necked flask and 60 mL of NaOH (2 mol/L) solution was added. The flask was placed in an oil bath at 100 °C to maintain reflux for 3 days. Then cooled to room temperature, the filter cake was collected by filtration, rinsed with anhydrous

methanol, and dried in a vacuum oven at 60 °C for 6 h, the TcCoPcTs solid with bright purple color was successfully prepared. In order to control variables and comparison, TcCoPcTs was further adjusted to tetra-β-carboxylate cobalt phthalocyanine (TcCoPc). The synthesis method is as follows: a certain amount of TcCoPcTs was dissolved in deionized water, and 1mol/L HCl solution was added to adjust the pH to 2-3. The precipitate was washed to neutrality by centrifugation, the product was collected by drying, and the TcCoPc was obtained. Yield: 66.4%. UV-vis spectra in DMF: λ_{max} (nm) = 668, 605. FT-IR spectra (KBr pellets) ν: 3699, 1700, 1522, 1333, 1150, 1089, 944, 741 cm^{-1}.

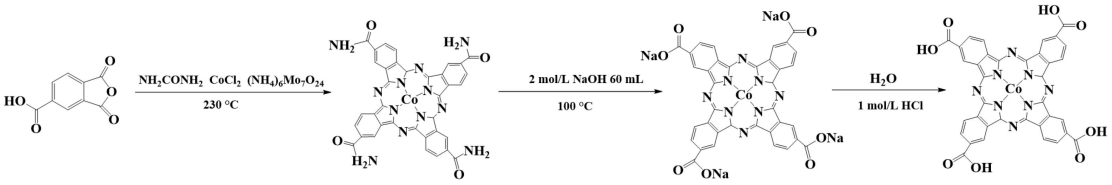

Scheme S1. Synthetical process of TcCoPcTs and TcCoPc

Synthesis of PPy NPs.

The freshly distilled Py monomer (1.2 mmol) was dissolved in 2 mL of isopropanol and recorded as group A. Ammonium persulfate (APS, 1:1 molar ratio of APS to Py) were ultrasonically dispersed in 4 mL of deionized water, designated as group B. All the above solutions were under the condition of 0-5 °C ice bath. The group B were added to group A and continuously stirred for 8 h under an ice bath. Finally, the reaction solution was filtered and washed with deionized water and ethanol until the filtrate was colorless, and dried under 60 °C for 2 h. The PPy black powder was obtained.

Synthesis of PPy/0.5TcCoPc hybrid.

The freshly distilled Py monomer (1.2 mmol) was dissolved in 2 mL of isopropanol and recorded as group A. TcCoPc (40:0.5 molar ratio of Py to TcCoPc) and ammonium persulfate (APS, 1:1 molar ratio of APS to Py) were ultrasonically dispersed in 4 mL of deionized water, designated as group B. All the above solutions were under the condition of 0-5 °C ice bath. The group B were added to group A and continuously stirred for 8 h under an ice bath. Finally, the reaction solution was filtered and washed with deionized water and ethanol until the filtrate was colorless, and dried under 60 °C for 2 h. The PPy/0.5TcCoPc black powder was obtained.

Result and discussion

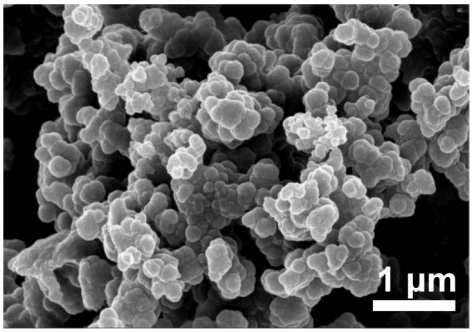

Fig. S1 SEM image of PPy NPs synthesized at 0-5 °C.

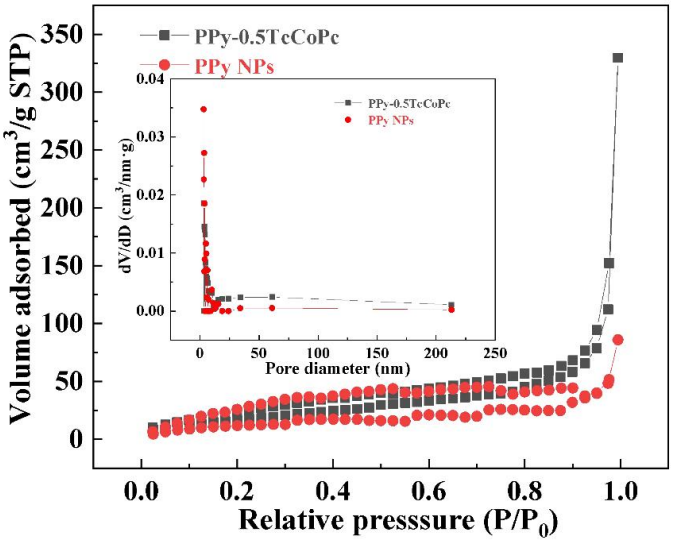

Fig. S2 N_2 adsorption − desorption isotherms and pore-size distribution curves (the inset) of the PPy NPs and PPy-0.5TcCoPc hybrid.

Table S1 Test data of N_2 adsorption – desorption for PPy-0.5TcCoPc, TcCoPc and PPy NPs.

Material	BET (m^2g^{-1})	Average pore diameter (nm)	Total pore volume (cm^3g^{-1})
PPy-0.5TcCoPc	66.94	30.54	0.51
TcCoPc	12.93	10.63	0.03
PPy NPs	43.62	12.19	0.13

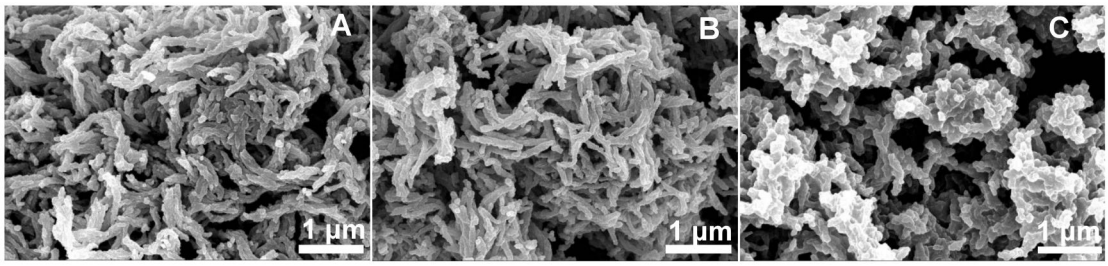

Fig. S3 Influence of different proportions on the morphology of PPy-TcCoPc. (A) PPy-1.0TcCoPc. (B) PPy-0.5TcCoPc. (C) PPy-0.25TcCoPc.

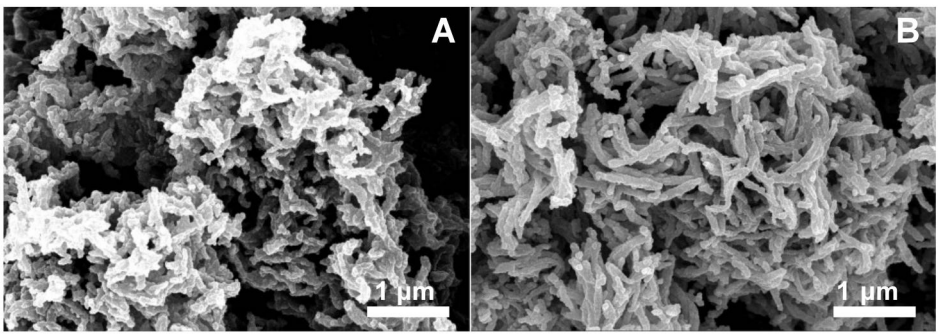

Fig. S4 Influence of temperature on the morphology of PPy-0.5TcCoPc: (A) 25 °C; (B) 0-5 °C

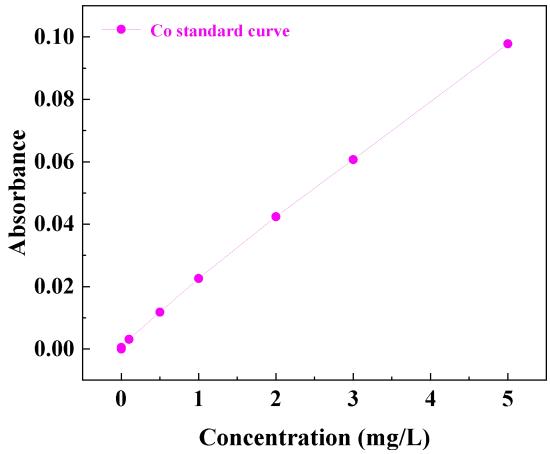

Fig S5 Cobalt Standard Curve of Flame Atomic Absorption

Table S2 TcCoPc content determination table in PPy-0.25TcCoPc, PPy-0.5TcCoPc, PPy-1.0TcCoPc by Flame Atomic Absorption

Material	Absorbance		Concentration of Co (mg/L)		Content of TcCoPc (%)
	Sample	Average	Sample	Average	
PPy-0.25TcCoPc	0.0136 0.0140 0.0141	0.0139	0.559 0.579 0.581	0.573	7.25
PPy-0.5TcCoPc	0.0292 0.0300 0.0299	0.0297	1.338 1.374 1.373	1.362	17.23
PPy-1.0TcCoPc	0.0347 0.0353 0.0355	0.0352	1.619 1.650 1.664	1.640	20.80

0, 0.2, 1, 2, 4, 6, 10 mL of the diluted cobalt standard solution (50 mg/L) was pipetted into a 100 mL volumetric flask, and 1% nitric acid solution was used to constant volume. The standard solution was injected into the test instrument, a cobalt atom standard curve was obtained. Subsequently, 5 mg of PPy-0.25TcCoPc PPy-0.5TcCoPc PPy-1.0TcCoPc were added to the into beakers, 6 mL of concentrated nitric acid and 2 mL of concentrated hydrochloric acid were sequentially added, and the nitration reaction was performed by heating to 100 °C. When the solution was clear and the powder was completely dissolved, the solution in the beakers was filtered into three 50 mL colorimetric tubes and constant volume. Finally, the test samples were injected into the test instrument and tested for three times to get the cobalt concentration average value of test sample. According to the law of conservation, 1 mol TcCoPc contains 1 mol Co atom. Based on this calculation, the content of TcCoPc in PPy-0.25TcCoPc, PPy-0.5TcCoPc and PPy-1.0TcCoPc were 7.25%, 17.23%, and 20.80%, respectively.

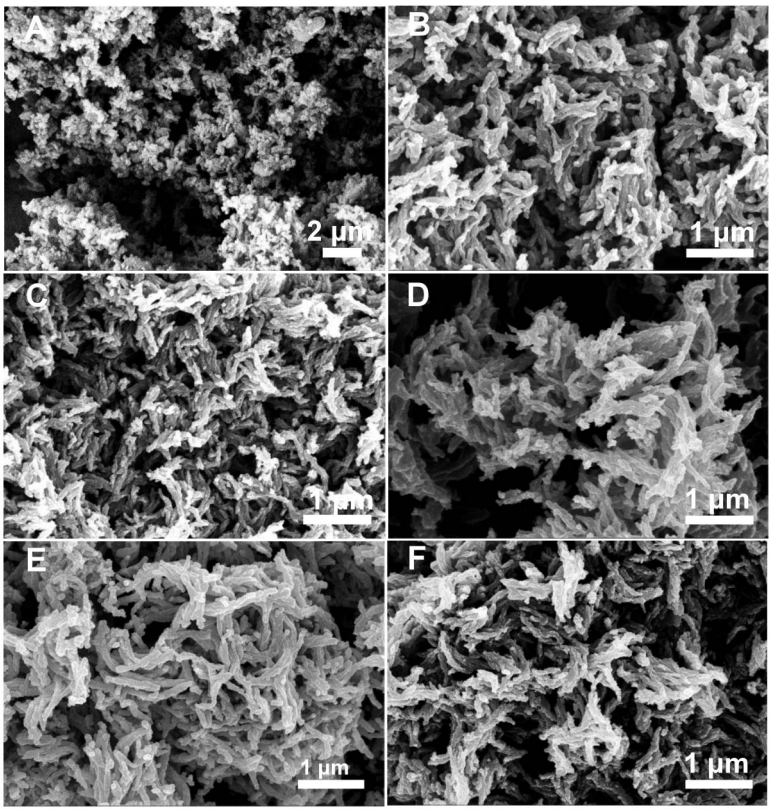

Fig. S6 Influence of different reaction time on the morphology of PPy-0.5TcCoPc: (A) Less than 2 min; (B) 10 min; (C) 1 h; (D) 4 h; (E) 8 h; (F) 16 h.

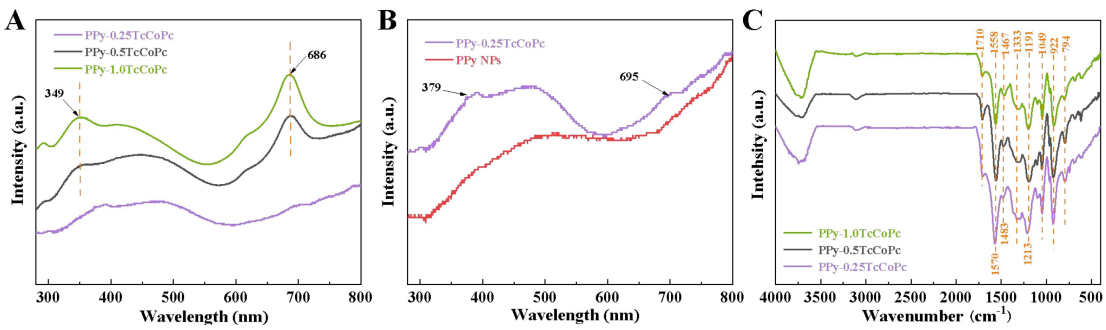

Fig. S7 (A) and (B) UV-vis spectra of PPy-0.25TcCoPc, PPy-0.5TcCoPc, PPy-1.0TcCoPc and PPy NPs. (C) FTIR spectra of PPy-0.25TcCoPc, PPy-0.5TcCoPc and PPy-1.0TcCoPc.

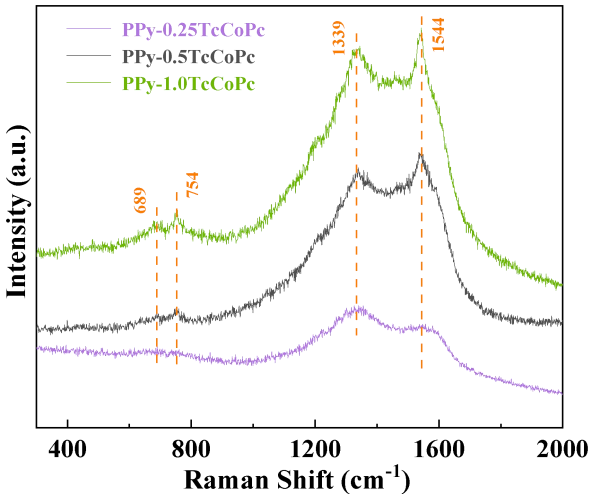

Fig. S8 Raman spectra of PPy-0.25TcCoPc, PPy-0.5TcCoPc and PPy-1.0TcCoPc hybrids obtained at λ_{exc} = 633 nm.

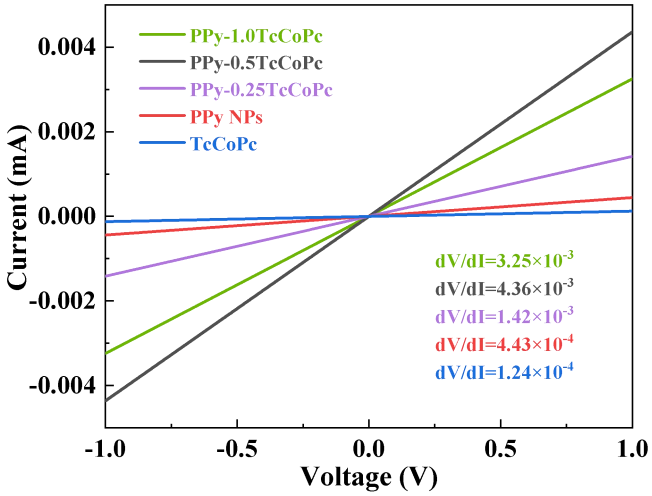

Fig. S9 *I*−*V* curves of PPy NPs, TcCoPc, PPy-0.25TcCoPc, PPy-0.5TcCoPc and PPy-1.0TcCoPc.

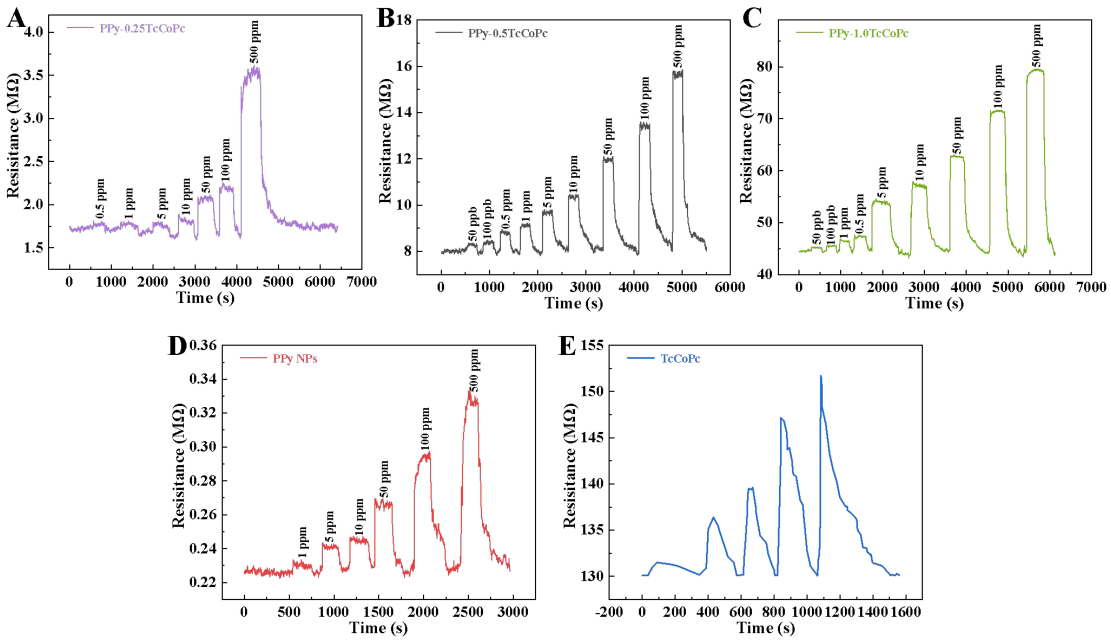

Fig S10 Response curve of the PPy-0.25TcCoPc, PPy-0.5TcCoPc, PPy-1.0TcCoPc, PPy NPs and TcCoPc sensors upon varying the concentration of NH_3.

Table S3 Comparison of the detection performances of PPy-0.25TcCoPc, PPy-0.5TcCoPc, PPy-1.0TcCoPc, PPy NPs and TcCoPc sensors upon exposure to different concentrations of NH_3 from 1 to 50 ppm.

Sensor Material	$\Delta R/R_a$ (%)/ Detection conc. (ppm)	Response time (s)/ Detection conc. (ppm)	Recovery time (min)/ Detection conc. (ppm)
TcCoPc	1.08/1 4.85/5 7.23/10 13.11/50	45.0/1 39.6/5 26.1/10 20.7/50	1.92/1 2.3/5 2.58/10 3.65/50
PPy NPs	1.11/1 4.61/5 8.8/10 18.55/50	58.5/1 50.4/5 43.2/10 28.8/50	2.48/1 4.27/5 5.15/10 6.88/50
PPy-0.25TcCoPc	5.22/1 5.89/5 8.39/10 23.01/50	67.5/1 45.0/5 36.9/10 28.8/50	1.53/1 1.73/5 1.83/10 2.39/50
PPy-0.5TcCoPc	**13.91/1** **20.62/5** **29.32/10** **49.32/50**	**13.5/1** **11.7/5** **8.99/10** **8.1/50**	**1.8/1** **3.9/5** **4.5/10** **6.1/50**
PPy-1.0TcCoPc	6.19/1 19.5/5 28.25/10 38.0/50	42.3/1 38.7/5 29.7/10 13.5/50	2.12/1 4.7/5 7.0/10 9.1/50

The LOD of the PPy-0.5TcCoPc sensor was calculated using the following equation [2-4]:

$$LOD_{ppm} = 3 \times \frac{RMS_{noise}}{slope} \qquad \text{(Eq. 1)}$$

Here, we took 600 data points before the sensor was exposed to ammonia gas and calculated the standard deviation (S). The following formula was used to calculate the RMS_{noise} of the sensor:

$$RMS_{noise}=\sqrt{\frac{S^2}{N}} \qquad \text{(Eq. 2)}$$

where N is the number of selected data points. According to the IUPAC definition, the signal-to-noise ratio is 3. Through Table 1, the slope value of the linear regression curve is obtained. Based on the above, the LOD of the PPy-0.5TcCoPc sensor was calculated to be 8.1 ppb.

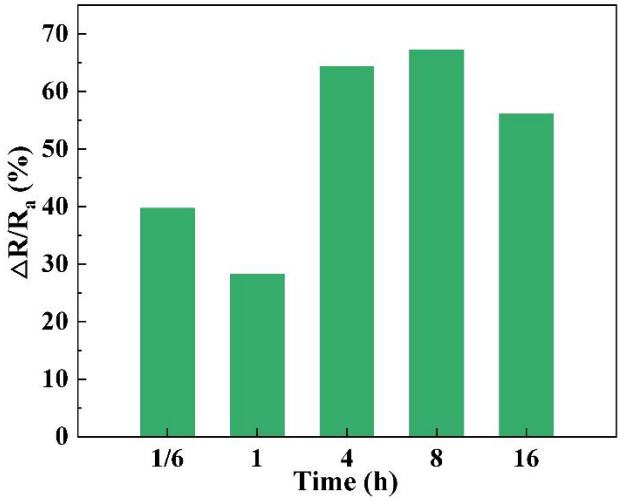

Fig S11 Influence of different reaction time on NH_3 sensing responses of PPy-0.5TcCoPc.

Table S4 Room-temperature NH_3-sensing properties of PPy-based sensors

Sensing Material	Response (%)/Detection conc. (ppm)[b]	Detection limit (ppm)[a]	Response time (s)/Detection conc. (ppm)[b]	Recovery time (s)/Detection conc. (ppm)[b]	Ref.
PPy–s-CoPc	3.6/45	25	60/45	240/45	5
PPy-(PAMPSNa)	5.83/52	25	429/52	-	6
DBSA-doped PPy–ZTO	5.44/27	5	288/27	76/27	7
PPy nanosheets films	12/50	5	240/50	3000/50	8
PPy/rGO	6.1/1	<1	60/ 1	300/1	9
PPy nanoparticles cluster PPy nanofibers matrix	115/350 71/350	1.156 1.153	10/350 7/350	44/350 90/350	10
PPy-shell@LNWs	10.1/10	0.13	-	-	11
PPy/SRGO	~6.8/10	0.0002	48/1	234/1	12
PPy/TiO_2/SiOC	18.67/50	10	119/50	86/50	13
rGO/$MoSe_2$	0.563/3	0.3	14/1	19/1	14
$Ti_3C_2T_x$/$Co(OH)_2$	14.7/100	<5	29/5	49/5	15
PPy-0.5TcCoPc	**49.32/50**	**0.0081**	**8.1/50**	**366/50**	**This work**

[a] If the sensor detection limit was not explicitly provided in the original report, then the lowest tested analyte concentration was listed.
[b] If the response (%), response time (s) or recovery time (s) of the sensor were not explicitly provided in the original report, then the estimate from the curve in that report was listed.

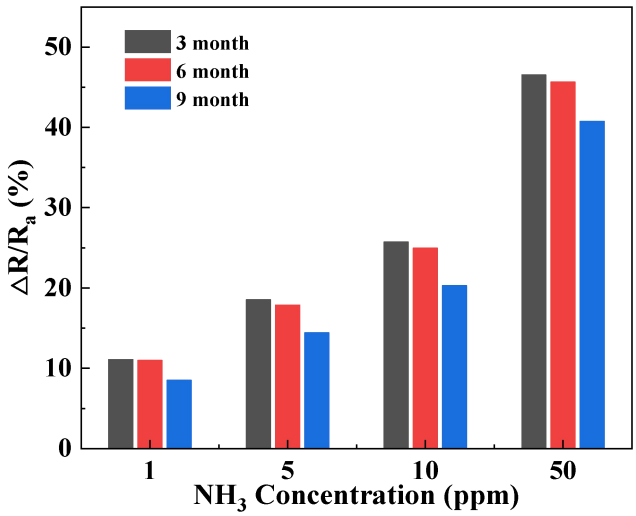

Fig. S12 Shelf life test of PPy-0.5TcCoPc sensor at 3, 6 and 9 months.

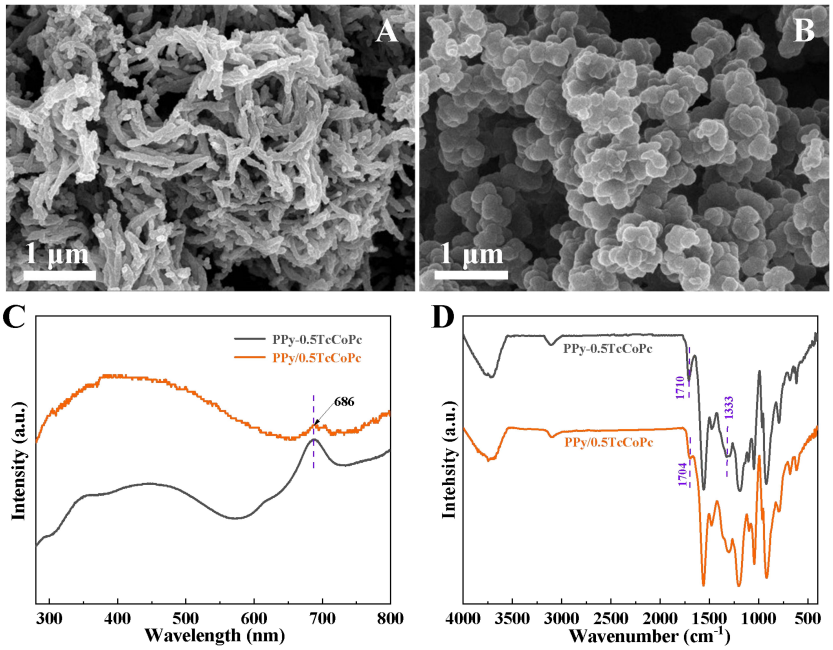

Fig. S13 (A and B) SEM of PPy-0.5TcCoPc and PPy/0.5TcCoPc hybrids. (C-D) UV-vis and FT-IR spectra of PPy-0.5TcCoPc and PPy/0.5TcCoPc hybrids.

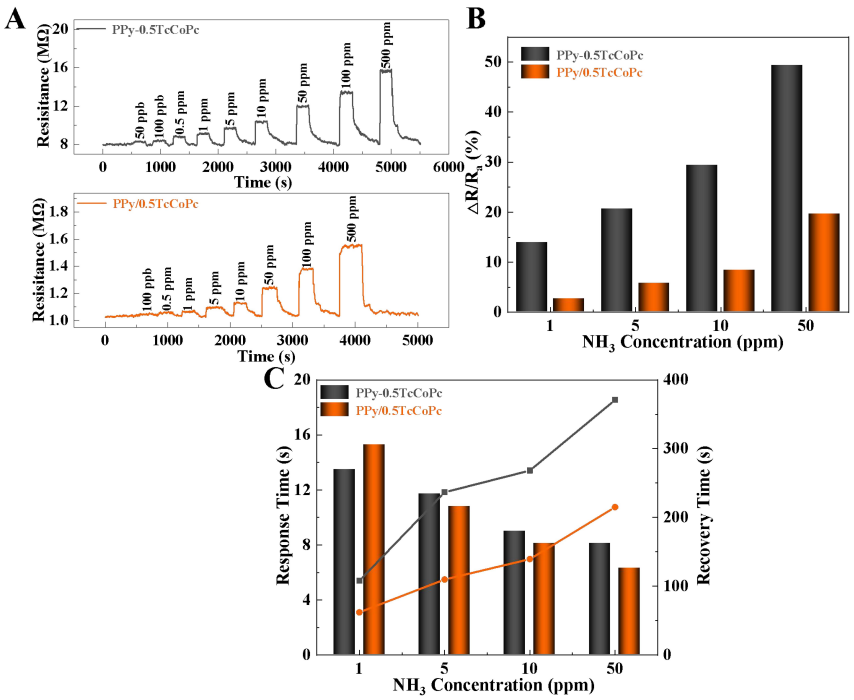

Fig. S14 NH_3-sensing properties and parameters of PPy-0.5TcCoPc and PPy/0.5TcCoPc sensors: (A) Response curve upon varying the concentration of NH_3. (B) NH_3 sensing response value of two sensors at 1, 5, 10, and 50 ppm. (C) Bar chart of response time and line chart of recovery time to NH_3.

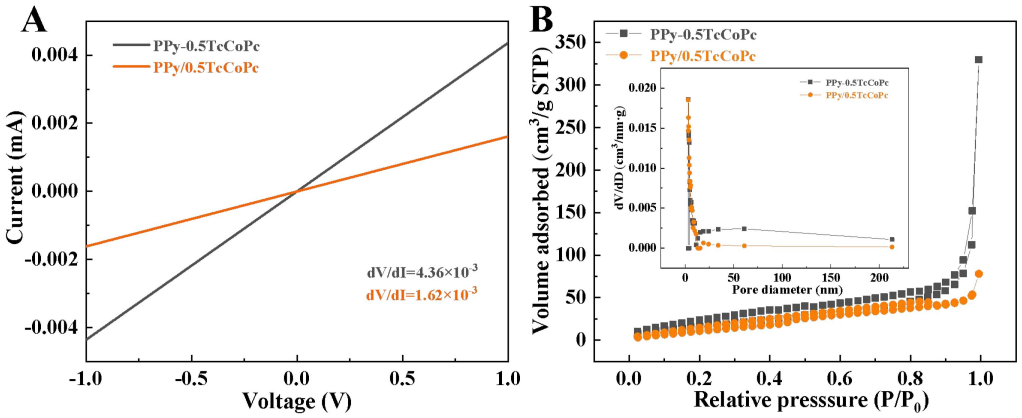

Fig. S15 (A) *I*−*V* curves and (B) N_2 adsorption − desorption isotherms and pore-size distribution curves (the inset) of the PPy-0.5TcCoPc and PPy/0.5TcCoPc hybrid, respectively.

Table S5 Test data of N_2 adsorption – desorption for PPy-0.5TcCoPc and PPy/0.5TcCoPc.

Material	BET (m^2g^{-1})	Average pore diamete (nm)	Total pore volume (cm^3g^{-1})
PPy-0.5TcCoPc	66.94	30.54	0.51
PPy/0.5TcCoPc	59.96	8.06	0.12

Reference:

1. H. Wu, Z. M. Chen, J. L. Zhang, F. Wu, C. Y. He, Z. Y. Ren and Y. Q. Wu, *Chem. Mater.*, 2017, **29**, 9509-9517.
2. Y. G. Wang, L. C. Yao, L. J. Xu, W. H. Wu, W. H. Lin, C. H. Zheng, Y. Q. Feng and X. Gao, *Sens. Actuators B Chem.*, 2021, **332**, 129497.
3. T. T. Nguyet, C. M. Hung, D. T. T. Le, N. V. Duy, N. D. Hoa, F. Biasioli, M. Tonezzer and C. Di Natale, *Ceram. Int.*, 2021, **47**, 28811-28820.
4. J. Li, Y. J. Lu, Q. Ye, M. Cinke, J. Han and M. Meyyappan, *Nano Lett.*, 2003, **3**, 929-933.
5. T. Sizun, T. Patois, M. Bouvet and B. Lakard, *J. Mater. Chem.*, 2012, **22**, 25246-25253.
6. O. L. Gribkova, V. A. Kabanova and A. A. Nekrasov, *J. Solid State Electr.*, 2020, **24**, 3091-3103.
7. S. A. H. Juybari and H. M. Moghaddam, *Mod. Phys. Lett. B*, 2020, **34**, 2050188.
8. P. Jha, N. S. Ramgir, P. K. Sharma, N. Datta, S. Kailasaganapathi, M. Kaur, S. P. Koiry, V. Saxena, A. K. Chauhan, A. K. Debnath, A. Singh, D. K. Aswal and S. K. Gupta, *Mater. Chem. Phys.*, 2013, **140**, 300-306.
9. X. H. Tang, J. P. Raskin, N. Kryvutsa, S. Hermans, O. Slobodian, A. N. Nazarov and M. Debliquy, *Sens. Actuators B Chem.*, 2020, **305**, 127423.
10. H. T. Hien, C. V. Tuan, D. T. A. Thu, P. Q. Ngan, G. H. Thai, S. C. Doanh, H. T. Giang, N. D. Van and T. Trung, *Synthetic Met.*, 2019, **250**, 35-41.
11. Y. X. Qin, Z. Cui, T. Y. Zhang and D. Liu, *Sens. Actuators B Chem.*, 2018, **258**, 246-254.
12. A. Shahmoradi, A. Hosseini, A. Akbarinejad and N. Alizadeh, *Anal. Chem.*, 2021, **93**, 6706-6714.
13. S. X. Zhou, L. Yao, H. Mei, M. Y. Lu, L. F. Cheng and L. T. Zhang, *Compos. Part B-Eng.*, 2022, **230**, 109536.
14. R. Jha, A. Nanda and N. Bhat, *IEEE Sens. J.*, 2021, **21**, 10211-10218.
15. B. Huang, Z. H. Zhao, P. Chen, B. C. Zhou, Z. Chen, Y. Fu, H. Y. Zhu, C. Chen, S. W. Zhang, A. B. Wang, P. Shi and X. Q. Shen, *RSC Adv.*, 2022, **12**, 33056-33063.